

Phonon Scattering and Internal Friction in Dielectric and Metallic Films at Low Temperatures

P. D. Vu¹, Xiao Liu², and R. O. Pohl^{3,*}

¹*Soka University of America, Aliso Viejo, CA 92656*

²*SFA, Inc., Largo, Maryland 20774*

³*LASSP, Cornell University, Clark Hall, Ithaca, New York 14853-2501*

**email: pohl@ccmr.cornell.edu*

(October 30, 2018)

We have measured the heat conduction between 0.05 K and 1.0 K of high purity silicon wafers carrying on their polished faces thin dielectric films of *e*-beam amorphous Si, molecular beam epitaxial (MBE) Si, *e*-beam polycrystalline CaF₂, and MBE CaF₂, and polycrystalline thin metallic films of *e*-beam Al, sputtered alloy Al 5056, *e*-beam Ti, and *e*-beam Cu. Using a Monte Carlo simulation to analyze the conduction measurements, we have determined the phonon mean free path within the films, and found all of them to be much shorter even than in typical bulk amorphous solids, with no exceptions. We have also measured the internal friction of these films below 10 K and found, however, their internal friction at low temperatures strikingly close to that of amorphous solids, both in magnitude and in their temperature independence, with the exception of the MBE Si and alloy Al 5056, whose internal friction is even much smaller than that of amorphous solids. The internal friction results indicate the phonon scattering in these thin films is the same as, or even much less stronger than, in other amorphous solids, according to the Tunneling Model. Thus, we conclude that the heat conduction measurements do not support the picture that the lattice vibrations of these films are glasslike, as had been surmised earlier for thin metallic films, on the basis of low temperature internal friction measurements alone [Phys. Rev. B **59**, 11767 (1999)]. At the least, the films must contain additional scattering centers which lead to the very small phonon mean free path. Most remarkably, the MBE Si shows the same strong scattering of thermal phonons as do the other films, while having the negligible internal friction expected for a perfect film. The disorder causing the strong scattering of the thermal phonons in this film is completely unknown. The non-glasslike phonon scattering phenomena observed here in thin dielectric and metallic films deserve further investigations.

I. INTRODUCTION

Structure and perfection of thin films on substrates are still poorly understood. The purpose of the present investigation is to show that thermal phonons with wavelengths on the order of 100 nm can be used as very sensitive probes of their disorder. It will be shown that strong phonon scattering occurs in a large number of films, including silicon films produced on silicon substrates by molecular beam epitaxy (MBE). The nature of this disorder is, however, not understood.

It has recently been shown that the internal friction of crystalline metal films below 10 K resembles that of amorphous solids both in magnitude and temperature independence, the so-called internal friction plateau [1]. A possible explanation was that crystalline metal films have the same density of tunneling states as amorphous solids. In disordered crystals, such states are called glass-like excitations [2]. According to the Tunneling Model (TM) [3], both the low temperature thermal conductivity below 1 K and the internal friction plateau below 10 K are determined by the same quantity, the tunneling strength C :

$$C = \frac{\overline{P}\gamma^2}{\rho v_t^2}, \quad (1)$$

where \overline{P} is the uniform spectral density of the tunneling states, γ is their coupling energy to phonons, ρ is the mass density, and v_t is the transverse sound velocity. C determines the internal friction plateau through relaxational scattering of the elastic wave, and the phonon thermal conductivity through resonant scattering of the thermal phonons. This quantitative connection between internal friction and thermal conductivity has been proven in many cases for bulk amorphous solids and also for disordered crystals, and constitutes a major proof of the validity of the TM, as reviewed in Refs. [4] and [5].

We have recently described a technique by which we can measure thermal phonon scattering in thin films on substrates [6]. Using this technique, we have verified the quantitative connection between internal friction and thermal conductivity successfully for amorphous silica films [6] and for crystalline silicon layers which had been disordered by ion implantation to the point of amorphization [7]. We will use this technique here for a comparison with the internal friction on a variety of dielectric and metallic films. If the lattice vibration of the films are

TABLE I. Preparation parameters of the thin films used for the heat conduction measurements in this work. The Cu film has a thin (100 Å) adhesive layer of Ti between it and the silicon substrate. The alloy Al 5056 film contains, by weight, 5.2% Mg, 0.1% Mn, and 0.1% Cr. The films were deposited onto either one or both of the wide polished substrate faces (see Ref. [6]), as indicated in the last column ("one" or "both").

	deposition technique	base pressure (Torr)	substrate temperature (°C)	substrate orientation	deposition rate (Å/s)	film thickness (μm)
<i>a</i> -Si	<i>e</i> -beam	2×10^{-7}	room	$\langle 100 \rangle$	15	0.5, one
MBE Si	MBE	UHV	600	$\langle 100 \rangle$	3	0.4, one
CaF ₂	<i>e</i> -beam	1×10^{-6}	room	$\langle 111 \rangle$	10	0.1, both
MBE CaF ₂	MBE	UHV	750	$\langle 111 \rangle$	0.14-0.28	0.4, one
Al	<i>e</i> -beam	4×10^{-7}	room	$\langle 100 \rangle$	15	0.2, one 0.4, one 0.6, one
Al 5056	sputter	Ar: 1×10^{-2}	room	$\langle 100 \rangle$	12	0.5, one
Ti	<i>e</i> -beam	6×10^{-7}	room	$\langle 111 \rangle$	3	0.1, both
Cu	<i>e</i> -beam	2×10^{-6}	room	$\langle 111 \rangle$	6	0.1, both

indeed glass-like, the phonon scattering should be determined by the same tunneling strength as determined from the internal friction.

In addition to the phonon scattering in the metal films studied previously in internal friction [1], we will also present measurements of both internal friction and phonon scattering in amorphous Si (*a*-Si) films, in dielectric crystalline CaF₂ films, and in a crystalline Si film produced by MBE, which is expected to contain fewer defects than any of the other films.

II. EXPERIMENTAL MATTERS

A. Thin Films

The thin films for heat conduction measurements were deposited either on Czochralski-grown, $\langle 111 \rangle$ oriented silicon substrate surfaces, or on float-zone refined, $\langle 100 \rangle$ oriented ones. For internal friction measurements, the thin films were deposited onto the double-paddle oscillators, which were float-zone refined, $\langle 100 \rangle$ oriented. All substrates were of high purity, and were double-side polished. Film thickness was determined by calibrated vibrations of a 6 MHz plano-convex quartz crystal. When possible, it was double-checked with a step surface profiler. Details on the films for heat conduction measurements are contained in Table I.

In order to eliminate surface contaminations to thermal conduction measurements, samples were, when appropriate, either put through an RCA clean [8] or cleaned in a hot sulfuric acid solution [9]. For the internal friction measurements, all films were deposited directly onto

double-paddle oscillators after cleaning of the substrate by diluted HF solution, except for the MBE Si film. Because of the stringent cleaning requirements prior to the MBE deposition in the UHV chamber, which were not suitable for double-paddle oscillators, the MBE Si film was deposited onto a wafer from which an oscillator was subsequently fabricated. The fabrication process involves heating the wafer to 850°C for 20 minutes. Thus, the MBE Si film for the internal friction measurement was considered as annealed. All the other annealing processes were done in the MOS area of the Cornell Nanofabrication Facility and were preceded by a stringent RCA cleaning, as described in Ref. [10], in order to avoid any contamination of the silicon which is known to occur during annealing under regular clean laboratory conditions. This annealing process will be referred to in the following as "MOS-cleaned-and-annealed."

Since we are primarily interested in the thermal phonon mean free path in the film from the heat conduction measurement, we would like to minimize phonon scattering at the film-substrate interface and at the free surface of the film. As the film-substrate interface is expected to be much smoother than the free surface of the film, we first consider the free surface roughness of the films studied in this work. Table II presents the root-mean-square (RMS) roughness of the free surfaces of the films studied as determined by atomic force microscopy (AFM). Table II also presents the dominant thermal phonon wavelength at 1 K based on the Debye speed of sound of the materials listed. The wave length of the thermal phonons is the relevant length. As can be seen, the RMS roughness is small compared to the length scale of the thermal phonons; and so, the free surfaces of the

TABLE II. Comparison of the free surface RMS roughness as determined by AFM measurements with the dominant thermal phonon wavelength λ_{dom} at 1 K based on the Debye speed of sound, v_D , for the thin film samples studied.

	film thickness (μm)	v_D^a (10^5 cm/s)	λ_{dom} at 1 K (\AA)	RMS Roughness (\AA)
<i>a</i> -Si	0.5	4.62	510	5
MBE Si	0.4	5.93	650	< 2
CaF ₂	0.1	4.10	450	25
MBE CaF ₂	0.4	4.10	450	7
Al	0.2	3.42	370	40
	0.4	3.42	370	20
	0.6	3.42	370	40
Al 5056	0.5	3.42	370	40
Ti	0.1	3.48	380	10
Cu	0.1	2.78	300	10

^a Taken from Ref. [11] or estimated using Eq. 6 with v_t listed in Table III.

films should have little effect on the overall scattering of thermal phonons and thus on the overall conclusions of this work. In section III C, we will show experimental evidence that phonon scattering at the surfaces/interfaces is indeed negligible relative to that in the films, by studying films thickness dependence.

B. Methods

In contrast to the conventional thermal conductivity measurements on bulk metals, our thermal method, as applied to metal films, has the advantage of solely determining the phonon heat transport in the form of a phonon mean free path in the film. In our investigation the metal films act primarily as phonon scatterers rather than as heat conductors because of their relatively small thickness to that of the substrate. At low temperatures, most of the heat in normal metals is carried by electrons. This thermal conductivity can be calculated using the Wiedemann-Franz-Lorenz law (reviewed in Ref. [12]) and an appropriate electrical resistivity. Because heat transport is parallel to the film-substrate interface, the amount of heat carried by the film or the substrate depends on their relative thermal resistance, which is the inverse of thermal conductivity multiplied by length and divided by cross-sectional area. Since the film and substrate have the same length and width and differ only in thickness, a comparison of the products of thermal conductivity and thickness is enough to determine which carries most of the heat, which is shown in Fig. 1 using a $0.2\text{ }\mu\text{m}$ thick Cu film as an example. The low temperature thermal conductivity of the Cu film was determined with the

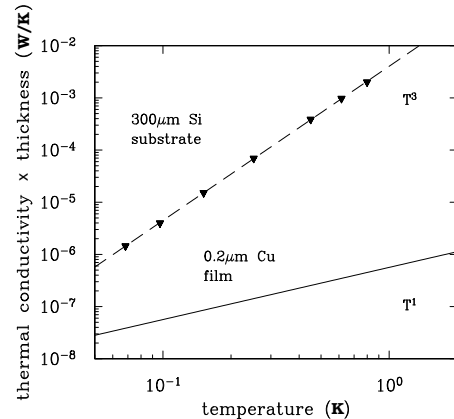


FIG. 1. Measured thermal conductivity of a high purity Si substrate (large faces polished and thin faces sandblasted, see Appendix) multiplied by its thickness, $300\text{ }\mu\text{m}$: solid triangles; and the calculated electronic thermal conductivity of a Cu film (see text) multiplied by its thickness, $0.2\text{ }\mu\text{m}$: solid line. At 50 mK, only about 5% of the heat is carried in the film (by electrons); at higher temperatures, the percentage drops as T^{-2} .

Wiedemann-Franz-Lorenz law using a room temperature electrical resistivity of $1.6 \times 10^{-6}\text{ }\Omega\text{cm}$ and a residual resistivity ratio of 2, measured in our laboratory on similar films [1,13]. Fig. 1 demonstrates that the substrate phonons are the dominant heat carriers, primarily because the thickness of the substrate is so much greater than that of the film. The same is true for the other metal films studied in this work, even more so when they become superconducting in the temperature range investigated here.

Thermal phonon mean free paths were determined, using a Monte Carlo (MC) simulation, from heat conduction measurements between 0.05 and 1.0 K by the technique described in Ref. [6], denoted as $\ell_{\text{film(HC)}}$ in the following. We mention briefly that additional scattering mechanisms such as scattering from free surface roughness can be included in the simulations, should that become necessary. For those who wish to determine $\ell_{\text{film(HC)}}$ from heat conduction measurements below 1 K without having to resort to performing their own simulations, we provide information in the Appendix, using the results of our MC simulations on a film-substrate sample with dimensions as typically used in our work.

We can also predict the phonon mean free path from internal friction measurements, denoted as $\ell_{\text{film(TM)}}$, if we assume that the film has the low energy excitations that are common in amorphous solids (and no other scattering centers) within the TM model. In the present work, the low-temperature internal friction of thin films is measured with double-paddle oscillators vibrating in their antisymmetric mode at $\sim 5.5\text{ kHz}$, which have exceptionally small background damping as described pre-

viously [14,15]. Thin films increase the internal friction of the paddle oscillator, Q_{paddle}^{-1} . From this, the internal friction of the film, Q_{film}^{-1} , is determined by [14]

$$Q_{\text{film}}^{-1} = \frac{G_{\text{sub}} t_{\text{sub}}}{3G_{\text{film}} t_{\text{film}}} (Q_{\text{paddle}}^{-1} - Q_{\text{sub}}^{-1}), \quad (2)$$

where t and G are thicknesses and shear moduli of substrate and film, respectively, and Q_{sub}^{-1} is the internal friction of the bare paddle (including the mounting losses). G_{film} is assumed to be equal to that of the bulk material [1,14]. The specific model used to obtain $\ell_{\text{film(TM)}}$ from the internal friction of a film is the TM, originally proposed by Anderson, et al. [16], and independently by Phillips [17], expanded for elastic measurements by Jäckle [18]. The TM connects the thermal phonon mean free path, ℓ , with the internal friction plateau, Q_0^{-1} , as follows. From Ref. [5], the expression for the thermal conductivity Λ is

$$\Lambda = \frac{1}{3} C_v v_D \ell = \frac{2.66 k_B^3}{6\pi \hbar^2} \frac{\pi}{2Q_0^{-1} v_t} T^2 \quad (3)$$

where, in the gas-kinetic picture, C_v is the low temperature specific heat per unit volume, v_D is the Debye speed of sound, k_B is Boltzmann's constant, \hbar is Planck's constant, and T is the temperature. Note that

$$Q_0^{-1} = \frac{\pi}{2} C, \quad (4)$$

where C is defined in Eq. 1. Substituting for C_v within the Debye model of the phonon spectrum [19], Eq. 3 becomes

$$\ell = (1.59 \times 10^{-12} [\text{s K}]) \frac{v_t}{Q_0^{-1}} T^{-1}, \quad (5)$$

assuming the empirical relation [11,20]:

$$v_t \simeq 0.9 v_D, \quad (6)$$

where [s K] are units of second and Kelvin. These equations provide the means to predict (within the TM) what $\ell_{\text{film(TM)}}$ should be if the internal friction plateau of the film, Q_0^{-1} , is known. To repeat, Eq. 5 assumes that the internal friction plateau is due to the presence of glassy states in the film, and that no defects other than the glass-like excitations scatter the thermal phonons. The validity of these assumptions will be tested for the films investigated here by comparing $\ell_{\text{film(HC)}}$ with $\ell_{\text{film(TM)}}$.

III. RESULTS AND DISCUSSION

A. Silicon Films

Since we are searching for tunneling states in thin films, we start with e -beam a -Si, a highly disordered film known

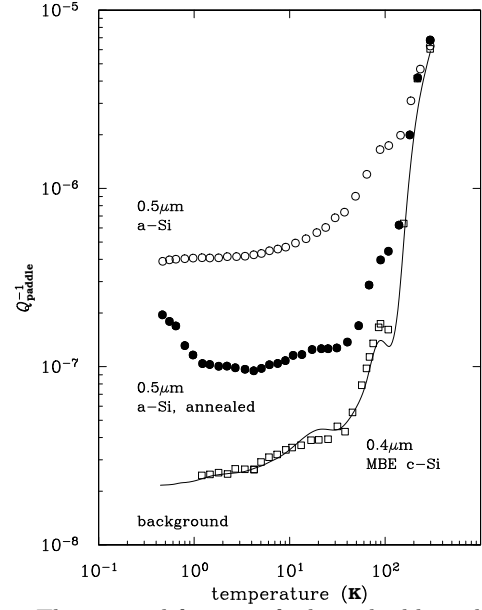


FIG. 2. The internal friction of a bare double-paddle oscillator (solid curve “background”) and of such oscillators carrying e -beam a -Si and MBE Si films. Note the negligible effect of the MBE film. The annealing of the e -beam a -Si film was done at 700°C for 1 hr under the MOS-cleaned-and-annealed condition (see text). The MBE Si film had been annealed at 850°C for 20 min (see text).

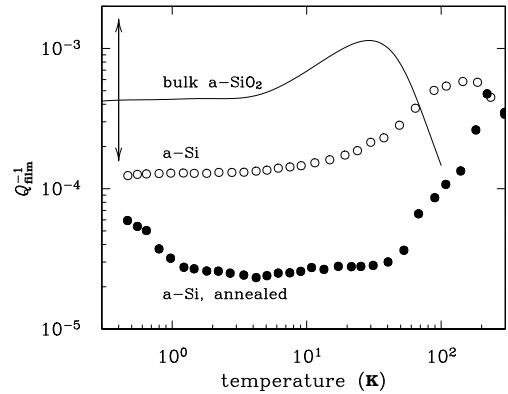


FIG. 3. Internal friction of an e -beam a -Si film, before and after annealing, compared to that of bulk a -SiO₂ (solid curve). The bulk a -SiO₂ data, measured at 4.5 kHz, are taken from J.E. Van Cleve, Ph.D. thesis, Cornell, published in Ref. [4]. The double-headed vertical arrow indicates the range of the temperature-independent internal friction plateau, measured on a wide range of bulk amorphous solids as reviewed in Ref. [5].

to have such states [14], and will compare it with a crystalline silicon film produced by MBE which is expected to be a simple extension of the silicon lattice. Fig. 2

shows the internal friction of a bare double paddle oscillator, called “background,” and of the same kind of oscillator carrying the films. As expected, the MBE film has negligible internal friction, while the *e*-beam *a*-Si films, both as-deposited and annealed, lead to a considerable increase of the internal friction. The MBE Si was measured only in the annealed state as explained in Section II A.

From the change of the internal friction of the paddle carrying the films, the internal friction of the films, Q_{film}^{-1} , can be determined using Eq. 2, and is compared to that of bulk *a*-SiO₂ in Fig. 3. The annealing of the *e*-beam film causes almost an order of magnitude reduction in Q_{film}^{-1} , while the Q_{film}^{-1} of the annealed MBE film is too small to be determined. Annealing at 700°C for 1 hr leads to almost complete crystallization of a 0.5 μm thick *e*-beam *a*-Si film [21]. The internal friction confirmed that $\sim 90\%$ of the low energy excitations had been removed. Below 1.0 K, however, the internal friction increased, indicative of a contamination in *c*-Si [10], although the most stringent MOS-cleaned-and-annealed process, as described in Section II A, was strictly followed. Most probably, an impurity was trapped on the substrate surface during mounting in the *e*-beam evaporator which is located outside the MOS area. This impurity, trapped underneath the *a*-Si film, survived the MOS cleaning and led to the contamination during the annealing. In contrast, there is no such problem for the MBE Si film, and hence no contamination is observed.

Table III summarizes Q_{film}^{-1} , v_t , $\ell_{\text{film(TM)}}(T)$ given by Eq. 5, for the films presented here and below. This en-

TABLE III. The internal friction plateau Q_{film}^{-1} , the transverse speed of sound v_t , and the thermal phonon mean free path $\ell_{\text{film(TM)}}(T)$ predicted by Eq. 5, where T is measured in Kelvin.

	Q_{film}^{-1}	v_t (10^5 cm/s)	$\ell_{\text{film(TM)}}(T)$ (μm)
<i>a</i> -Si	1.3×10^{-4}	4.16^b	$50.9/T$
annealed <i>a</i> -Si	2.4×10^{-5}	5.33^c	$353/T$
MBE Si	negligible	5.33^c	e
CaF ₂	6.0×10^{-5}	3.69^c	$97.8/T$
Al	1.0×10^{-4} ^a	3.04^c	$48.3/T$
Al 5056	1.0×10^{-5} ^a	3.04^c	$483.4/T$
Ti	2.0×10^{-4} ^a	3.13^d	$24.9/T$
Cu	5.3×10^{-4} ^a	2.50^c	$7.5/T$

^a Taken from Ref. [1]

^b Taken from Ref. [14]

^c Taken from Ref. [20]

^d Taken from Ref. [22]

^e There is no Q_{film}^{-1} value for the MBE Si film because the internal friction of this film was not detectable (see Fig. 2), and hence $\ell_{\text{film(TM)}}$ is expected to be very long.

ables us to compare the internal friction and the phonon mean free path directly within the TM.

Fig. 4 shows $\ell_{\text{film(HC)}}$ in the MBE Si and *e*-beam *a*-Si films both in as-deposited and annealed states obtained from the heat conduction measurements. The dotted line represents $\ell_{\text{film(TM)}}$ of the *e*-beam *a*-Si based on the internal friction measurement (see Table III). For *e*-beam *a*-Si, $\ell_{\text{film(HC)}}$ is significantly smaller than $\ell_{\text{film(TM)}}$ which assumes that the scattering occurs by tunneling states alone. Evidently, $\ell_{\text{film(HC)}}$ cannot be used to test for the existence of glassy excitations in *e*-beam *a*-Si film. In addition to the tunneling states, other scattering centers must be present. The situation may be similar to *e*-beam *a*-SiO₂ films in which the additional thermal phonon scattering was explained by cracks or voids [6]. It is well known that *a*-Si films produced by *e*-beam evaporation contain similar defects [23–25]. After annealing, only a small increase of $\ell_{\text{film(HC)}}$ above 0.3 K and even a decrease below that temperature can be seen in Fig. 4. This change of $\ell_{\text{film(HC)}}$ upon annealing, which cannot be explained within the TM, is interpreted as resulting from a combination of a decreased scattering by the tenfold smaller number of tunneling states, an increased scattering by the contaminants, and possibly a change in scattering from the defects of unknown nature which had been noticed already in the film prior to annealing. Obvi-

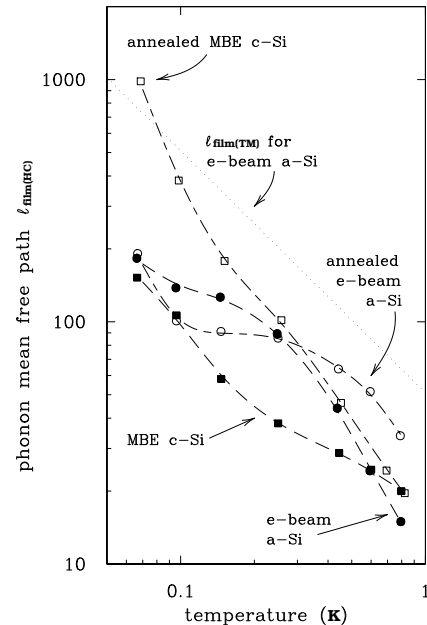


FIG. 4. Phonon mean free path $\ell_{\text{film(HC)}}$ of as-deposited and annealed silicon films. As-deposited *e*-beam *a*-Si: solid circles; annealed (700°C, 1 hr) *e*-beam *a*-Si: Open circles; as-deposited MBE Si: solid squares; annealed MBE Si (500°C, 1 hr followed by 700°C, 1.5 hrs): Open squares. The dotted line is $\ell_{\text{film(TM)}}(T)$, the TM prediction based on the internal friction plateau of the as-deposited *e*-beam *a*-Si. Dashed lines are guides for the eye.

ously, these results cannot be used to extract any knowledge about the annealing of these unknown defects. They do, however, provide further evidence for the presence of the contaminants introduced into crystalline silicon during annealing under all but the most stringent conditions, thus further emphasizing the need for their identification and control [10].

Very surprisingly, Fig. 4 shows that the phonon scattering in MBE Si film both before and after annealing is very large as well. Since the contamination that plagued the *e*-beam *a*-Si films is not an issue here, secondary ion mass spectroscopy (SIMS) was performed by R. Reedy at the National Renewable Energy Laboratory (NREL) in order to identify other possible chemical impurities. The following chemical elements were detected: boron, $< 10^{16} \text{ cm}^{-3}$; nitrogen, $\sim 3 \times 10^{16} \text{ cm}^{-3}$; carbon, $\sim 3 \times 10^{17} \text{ cm}^{-3}$; and hydrogen, $\sim 2 \times 10^{18} \text{ cm}^{-3}$. These concentrations were similar in the MBE film and the silicon substrate. Only the oxygen contents differed between substrate ($\sim 5 \times 10^{17} \text{ cm}^{-3}$) and film ($\sim 5 \times 10^{18} \text{ cm}^{-3}$). For all these detected impurities, an anneal (500°C, 1 hr followed by 700°C, 1.5 hr) caused no measurable change of their concentrations. Since no evidence for such scattering was observed on bare silicon samples from the same batch as used in these experiments [6], the only possible impurity scatterer is the oxygen. But the ten-fold increase of oxygen in the MBE film should not lead to a noticeable decrease of the experimental mean free path ℓ (defined in the Appendix, Eq. 7), and thus to a decrease of $\ell_{\text{film(HC)}}$ given the relatively small thickness of the film, unless the oxygen in the film somehow acts as a much stronger scattering center. Phonon scattering in oxygen-doped silicon has been found to depend on heat treatment [26,27] at frequencies in excess of $\sim 300 \text{ GHz}$. But, phonons in this frequency range carry heat predominantly above 3 K, and no evidence exists for phonon scattering by oxygen at lower frequencies (corresponds to $T < 1 \text{ K}$).

In an attempt to detect any evidence for structural disorder in this MBE film, an x-ray diffraction (XRD) analysis was performed by M. Sardela and D. Cahill at the University of Illinois (Champaign-Urbana). High resolution open-detector scans around the Si(004) peak showed no difference between measurements conducted on the film side and on the substrate side of the MBE Si film-substrate sample. Full width at half maximum values were found to be almost identical on both sides, and no diffuse scattering or any disorder feature on the film side was seen. In addition, a triple axis reciprocal space map around the Si(004) peak on the film side also could not detect any diffuse distribution nor asymmetry of the Si peak. These observations speak against the existence of grains with different orientations which might cause the phonon scattering.

The near T^{-1} temperature dependence may be suggestive of scattering by sessile dislocations as reported,

for example, by Wasserbäch in plastically deformed bulk copper, niobium, and tantalum [28]. If we assume that the coupling between dislocations and phonons is similar, the dislocation density in the MBE film would have to range between 10^{10} and 10^{13} cm^{-2} , which seems rather high for MBE silicon. At this point, no search for dislocations in this MBE film has been undertaken.

MOS-cleaning-and-annealing of the MBE film as described above leads to an increase of $\ell_{\text{film(HC)}}$ shown in Fig. 4, although it remains below the mean free path predicted even for *e*-beam *a*-Si, except at the lowest temperature. Thus, noticeable disorder, other than the tunneling states, remains in the MBE Si film even after annealing, although the internal friction of the annealed MBE Si film shown in Fig. 2 give no evidence for any low energy excitations. Thus, the only firm conclusion we can draw at this point is that the defects in the MBE film are not glass-like.

B. CaF₂ Films

As was just shown, crystalline films produced by crystallizing an *a*-Si film or by MBE deposition show little or no evidence for tunneling states in low temperature internal friction. It is therefore surprising that a $0.6 \mu\text{m}$ thick film of crystalline *e*-beam CaF₂ increases the damping of the double paddle oscillator by more than one order of magnitude, see Fig. 5. The internal friction of the film itself, as compared with that of *a*-SiO₂ shown in Fig. 6, is nearly temperature independent and close to the range found for all amorphous solids studied to date (with the exception of certain hydrogenated *a*-Si films, as discussed in Ref. [14]). Thus, the large internal friction observed previously in polycrystalline metal films [1] apparently also occurs in some crystalline dielectric films. Assuming that its cause is glass-like excitations, we can again predict an $\ell_{\text{film(TM)}}$ for the CaF₂ film, shown as the dotted line in Fig. 7. The measured $\ell_{\text{film(HC)}}$ for an identical CaF₂ film, also shown in Fig. 7, is more than two orders of magnitude smaller than predicted by the TM. We also measured the phonon mean free path of another crystalline CaF₂ film which was prepared by MBE technique at 750°C substrate temperature to improve its structure. However, the internal friction of the MBE CaF₂ film cannot be measured because of the difficulty of preparing such a film on silicon paddle oscillators and meeting the requirements of special cleaning and fabrication at the same time. The $\ell_{\text{film(HC)}}$ of the MBE CaF₂ film, though larger than that of the *e*-beam one, is still smaller than that predicted by the TM for the *e*-beam CaF₂ film. Furthermore, it is smaller than that of an *a*-SiO₂ film prepared by wet-thermal oxidation, in which the structure is much improved in comparison with *e*-beam *a*-SiO₂, and the phonon scattering is determined solely by the glassy excitations. The

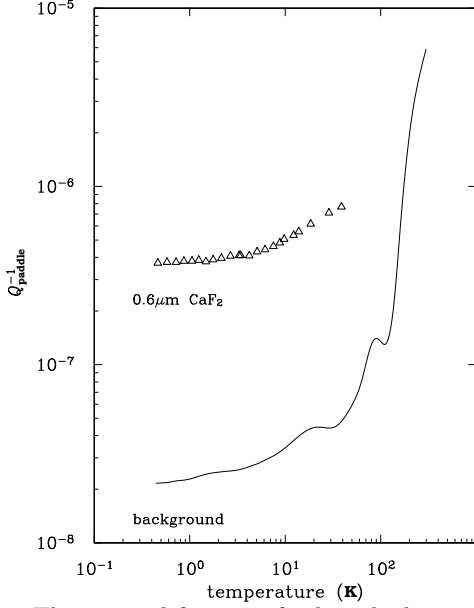


FIG. 5. The internal friction of a bare high purity silicon double-paddle oscillator (solid curve “background”) and of such a paddle carrying the *e*-beam CaF_2 film on the polished silicon surface.

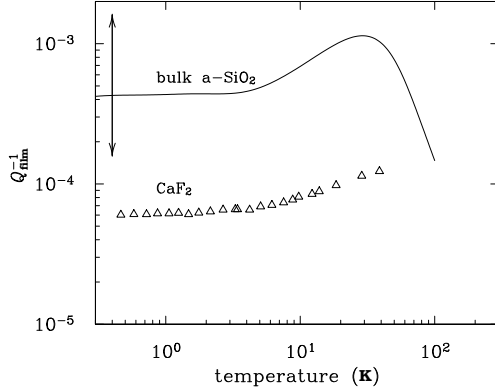


FIG. 6. Internal friction of the *e*-beam CaF_2 film compared to that of bulk $\alpha\text{-SiO}_2$ (solid curve). The bulk $\alpha\text{-SiO}_2$ data, measured at 4.5 kHz, is taken from J.E. Van Cleve, Ph.D. thesis, Cornell, published in Ref. [4]. The double-headed vertical arrow indicates the range of the temperature-independent internal friction plateau, measured on a wide range of bulk amorphous solids as reviewed in Ref. [5].

$\ell_{\text{film(HC)}}$ of the thermal $\alpha\text{-SiO}_2$ film agrees perfectly with that of the TM’s prediction, just as one would expect for bulk $\alpha\text{-SiO}_2$, as shown in Fig. 7 (see Ref. [6] for details). The $\ell_{\text{film(HC)}}$ of the MBE CaF_2 film locates between those of the thermal $\alpha\text{-SiO}_2$ film and a macroscopically as well as microscopically disordered *e*-beam $\alpha\text{-SiO}_2$ film, in which the thermal phonon scattering is not dominated by the tunneling states, also shown in Fig. 7. We suggest that this MBE CaF_2 film, al-

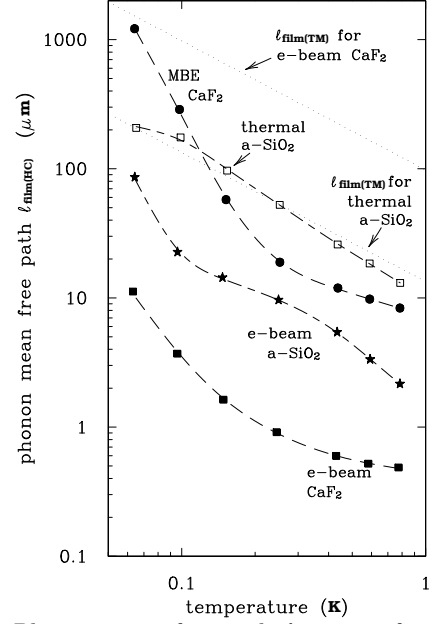


FIG. 7. Phonon mean free path $\ell_{\text{film(HC)}}$ of two different CaF_2 films. MBE CaF_2 : solid circles; *e*-beam CaF_2 : solid squares. The dotted lines are the TM prediction based on internal friction measurements for *e*-beam CaF_2 and for thermal $\alpha\text{-SiO}_2$, respectively. Data for the thermal (open squares) and *e*-beam (solid stars) $\alpha\text{-SiO}_2$ films are taken from Ref. [6]. For thermal $\alpha\text{-SiO}_2$, good agreement is shown between $\ell_{\text{film(HC)}}$ and $\ell_{\text{film(TM)}}$, which had also been found in ion-implanted silicon [7], as mentioned in Section I. Dashed lines are guides for the eye.

though probably more highly ordered than an *e*-beam one, contains disorder because the pseudomorphic epitaxial growth is known to break down at film thickness exceeding 10 nm [29,30], leading to structural relaxation. Internal stresses are also expected to result from differential thermal contraction as the sample is cooled from the deposition temperature. There is, however, no convincing evidence for glass-like excitations in this CaF_2 film. As in the *e*-beam $\alpha\text{-Si}$ film, some unknown scattering process masks the effect of the glass-like excitations, if they exist at all.

C. Metal Films

Fig. 8 shows $\ell_{\text{film(HC)}}$ for three *e*-beam Al films, 0.2, 0.4, and 0.6 μm thick. The absence of any significant dependence on the film thickness validates the assumption used in our analysis that the scattering occurs predominantly within the films and not at the interfaces, an assumption which so far had been based only on the smoothness observed on the free surfaces as listed in Table II. The dotted line is the prediction for $\ell_{\text{film(TM)}}$ based on the internal friction of the *e*-beam Al film reported

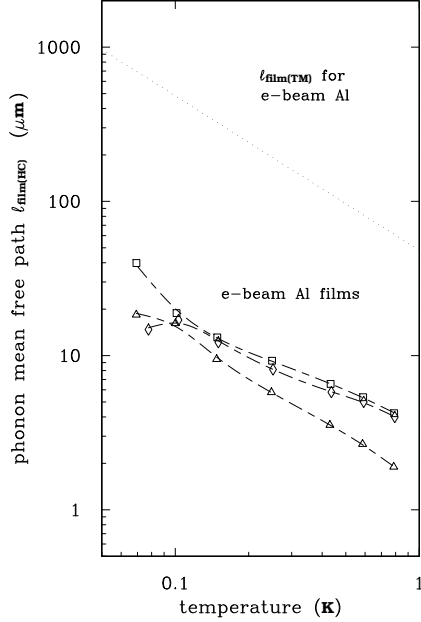


FIG. 8. Phonon mean free path $\ell_{\text{film(HC)}}$ for *e*-beam Al films that are 0.2 μm (open triangles), 0.4 μm (open squares), and 0.6 μm (open diamonds) thick. The dotted line is the TM prediction based on internal friction (see Table III). Dashed lines are guides for the eye.

earlier [1] (see also Table III). As for the two previous examples, the observed phonon scattering far exceeds the scattering expected on the basis of the TM.

In Ref. [1], it had been shown that the low temperature internal friction of an Al film on a Si substrate was very similar to that of heavily deformed bulk Al. It was therefore interesting to compare the phonon mean free path in the film with that observed in deformed bulk Al. For that purpose, a 99.999% pure polycrystalline Al rod (2.5 mm in diameter and 25.7 mm long) was first annealed at 560°C and subsequently stretched by 5%. Its thermal conductivity, measured by the standard steady-state technique, is shown in Fig. 9 along with that of bulk α -SiO₂. The steep rise of the thermal conductivity of the bulk Al above 0.1 K is caused by the onset of heat transport by normal state electrons. However, below that temperature, heat is expected to be carried predominantly by the lattice, and a temperature dependence similar to that of the bulk glass (α -SiO₂) is observed. Although the magnitude is three times smaller, it still falls within the glassy range in thermal conductivity, see Fig. 1 in ref. [31]. The phonon thermal conductivity of the 0.2 μm *e*-beam Al film, as calculated from $\ell_{\text{film(HC)}}$ in Fig. 8, is also shown in Fig. 9. Above 0.1 K, the thermal conductivity of the deformed bulk Al and the phonon thermal conductivity of the *e*-beam Al film show the difference between the heat transport by electrons and phonons, and by the phonons alone, separated here experimentally for the first time. Below 0.1 K, the phonon thermal conduc-

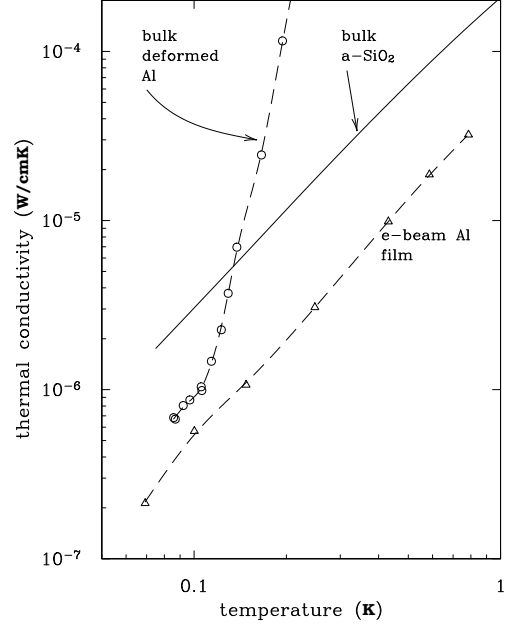


FIG. 9. The thermal conductivity of 5% deformed bulk Al. The thermal conductivity of a bulk α -SiO₂, taken from Ref. [32], along with the phonon thermal conductivity of the 0.2 μm thick *e*-beam Al film converted from their phonon mean free path shown in Fig. 8, is shown for comparison.

tivity of the *e*-beam Al film is very close to that of the deformed bulk sample. This suggests that the defects which scatter the phonons in the film are very similar to those in the heavily deformed bulk sample. The same conclusion had been reached previously in internal friction measurements as stated above. The defects causing the internal friction had been tentatively identified as dislocations or dislocation kinks [1]. It is tempting to suggest that the thermal phonons in the films are scattered by the same defects. Since we see in Fig. 8 that $\ell_{\text{film(HC)}}$ and $\ell_{\text{film(TM)}}$ of the *e*-beam Al films are not connected by the TM, we can conclude that the same holds for the deformed bulk Al because of the similarity in the internal friction and phonon mean free path between the thin films and the bulk samples. Thus, the non-glasslike phonon scattering phenomena observed in this work are not limited to thin films alone. In addition, the defects or the mechanisms causing the resonant scattering of thermal phonons in heat conduction and those leading to the relaxational process in internal friction may not even be related, as shown by the following observation.

The alloy Al 5056 in bulk form has an exceptionally small low temperature internal friction, even as a sputtered film (Table III), which has been explained by dislocation pinning [1]. The $\ell_{\text{film(HC)}}$ in this film, however, is still close to that of all other metal films, see Fig. 10. It follows that pinning of dislocations has no influence on the thermal

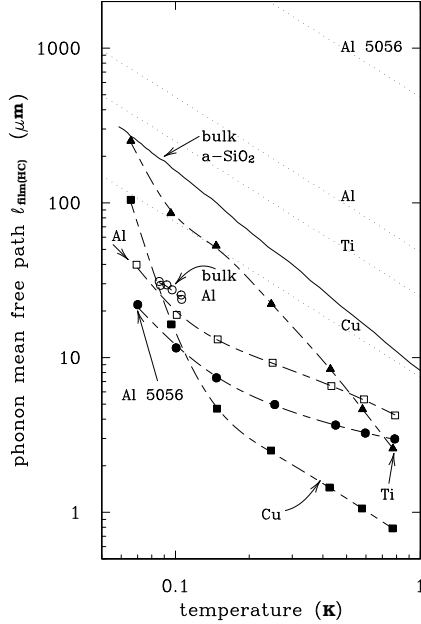


FIG. 10. Phonon mean free path $\ell_{\text{film(HC)}}$ for a $0.4 \mu\text{m}$ thick e -beam Al film: open squares; for a $0.5 \mu\text{m}$ thick sputtered alloy Al 5056 film: solid circles; for a $0.1 \mu\text{m}$ thick e -beam Ti film: solid triangles; and for a $0.1 \mu\text{m}$ thick e -beam Cu film: solid squares. The thermal conductivity of the 5% deformed bulk Al is converted to its mean free path: open circles. The labelled dotted lines are TM predictions of $\ell_{\text{film(TM)}}$ based on internal friction measurements (see Table III). The solid curve is the phonon mean free path in bulk $a\text{-SiO}_2$ taken from Ref. [32]. Dashed lines are guides for the eye.

phonon scattering. We conclude that the mechanisms causing the internal friction and the thermal phonon scattering are not understood.

A comparison between $\ell_{\text{film(HC)}}$ and $\ell_{\text{film(TM)}}$ is shown in Fig. 10 for four metal films: Al, alloy Al 5056, Ti, and Cu, with the phonon mean free path of $a\text{-SiO}_2$ for comparison. The apparent lack of correlation between $\ell_{\text{film(HC)}}$ and $\ell_{\text{film(TM)}}$ enable us to generalize the same conclusion from the Al films to other metallic films, which is that if glass-like lattice vibrations exist in them, their effect is masked by the unknown defects.

As observed in internal friction [1], $\ell_{\text{film(HC)}}$ is unaffected by superconductivity (T_c is 0.4 K for Ti, 0.92 K for alloy Al 5056 [33], and 1.2 K for Al,). It is concluded that phonon scattering by electrons is unimportant. Klemens has derived an expression for the phonon-electron scattering coefficient P in terms of the electron-phonon scattering coefficient E [34]. Using the value for E measured by Berman and MacDonald for pure copper [35,36], we calculate ℓ_{film} (of phonons being scattered by electrons) at 1 K to be $\sim 15 \mu\text{m}$. This phonon scattering rate (due to electrons) is more than an order of magnitude less than the phonon scattering rate observed in Fig. 10 for the Cu film. Note that the calculation of $15 \mu\text{m}$ should not be

taken too seriously as its assumptions [37] of the adiabatic principle, of a phonon Debye spectrum, and of a free electron gas may not be adequate at these temperatures for a thin polycrystalline Cu film with a residual resistivity ratio of 2 [1]. Nevertheless, this estimate agrees with our observation that electron-phonon interaction is not significant in our experiment.

IV. CONCLUSIONS

Measurements of the thermal phonon mean free path on films of amorphous and MBE Si, of polycrystalline and MBE CaF_2 , of pure metallic Al, Cu, and Ti, and of the metallic alloy Al 5056 below 1.0 K have revealed, in all cases, similar strong phonon scattering. Scattering by surface and interface roughness can be excluded, since nearly the same $\ell_{\text{film(HC)}}$ has been observed in Al films of different thicknesses. In searching for the origin of this phonon scattering, we have also measured the low temperature internal friction of the Si and CaF_2 films (that of the metal films had been measured previously, Ref. [1]) and also the thermal conductivity of a bulk Al rod after a 5% plastic elongation. In all cases, $\ell_{\text{film(HC)}}$ was found to be much smaller than $\ell_{\text{film(TM)}}$ based on the internal friction and assuming that the lattice vibrations are glass-like. The discrepancy is particularly striking for the MBE Si film in which no internal friction was observed, yet $\ell_{\text{film(HC)}}$ was similar to that found in all other films. In this case, the phonon scattering is particularly puzzling since the film is expected to be structurally more perfect. In all other films, macroscopic defects like grain boundaries, voids, cracks, or dislocations may be the cause for the phonon scattering. In the deformed bulk Al, the phonon mean free path was found to be equal to that in thin Al films. Since in the bulk sample, individual dislocations or aggregates thereof are likely phonon scatterers, they may also be the cause for the scattering in the films. However, dislocation motion, presumably tunneling, which has been invoked to explain the internal friction of deformed Al and of Al films (see Ref. [1,38]) is an unlikely cause for the thermal phonon scattering since the same $\ell_{\text{film(HC)}}$ in Al was also found in the alloy Al 5056, in which dislocation motion appears to be suppressed, resulting in a greatly reduced internal friction. In conclusion, both internal friction and phonon scattering have been shown to be sensitive probes for thin film disorder, including that in MBE Si. The nature of such disorder and the mechanisms by which it affects the elastic and thermal properties are completely unknown. No evidence for the existence of glass-like lattice vibrations has been detected.

Acknowledgements

We gratefully acknowledge the help of Aaron Judy with the AFM measurements, Glen Wilk in preparing the MBE Si film at Texas Instruments (Dallas), and Ken Krebs in fabricating the MBE CaF_2 film at the University of Georgia (Athens) and in providing very useful information on that film's defects. We thank Mauro Sardela and David Cahill for XRD analysis at the University of Illinois (Champaign-Urbana) and Bob Reedy for the SIMS investigation of the MBE Si film at the National Renewable Energy Laboratory. We also thank R.S. Crandall for fruitful discussions. This work was supported by the National Science Foundation, Grant No. DMR-9701972, the National Renewable Energy Laboratory, Grant No. RAD-8-18668, and the Naval Research Laboratory. Additional support was received from the Cornell Nanofabrication Facility, NSF Grant No. ECS-9319005, and the Cornell Center for Materials Research, Award No. DMR-9121564.

Appendix

The technique used in this investigation for the measurement of the thermal phonon mean free path in thin films has been described before [6]. Although the experimental schematic resembles that of a thermal conductivity measurement, see Fig. 11, it should be emphasized that our experiment leads directly to a thermal phonon mean free path, rather than to a thermal conductivity Λ , from which the mean free path ℓ has to be calculated using the gas-kinetic expression

$$\Lambda = \frac{1}{3} C_v \bar{v} \ell, \quad (7)$$

which requires knowledge of the specific heat C_v of the heat carrying excitations or phonons traveling with an average velocity \bar{v} . In amorphous solids, for example, this C_v cannot be measured. It can only be calculated from \bar{v} through the use of the Debye model.

The analysis of the heat conduction measurements on the silicon substrate carrying the film requires a Monte Carlo simulation which, though straightforward, is nonetheless time-consuming. By strictly adhering to the specifics as listed below (including sample and clamp geometry), one can extract the phonon mean free path in a film, ℓ_{film} (called $\ell_{\text{film(HC)}}$ in this paper), from ℓ_{exp} (the experimentally measured phonon mean free path of the film-substrate sample) without having to repeat any MC simulations, as will be shown in this Appendix.

Fig. 12 is a plot of the results of MC simulations on a film-substrate sample with dimensions typically used in this investigation. For any particular simulation, ℓ_{film}/x is an input parameter where x is the film thickness. The output parameter is ℓ_{MC} , a simulated phonon mean free path of the film-substrate sample. To determine ℓ_{film} , one sets an ℓ_{exp} equal to an ℓ_{MC} in Fig. 12 to find the

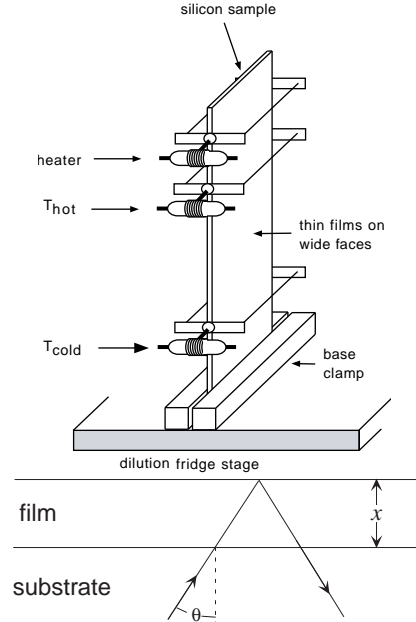


FIG. 11. Schematic of 1-D heat conduction experiment; the sample is cleaved from a high purity commercial silicon wafer (orientation $\langle 111 \rangle$ or $\langle 100 \rangle$) with both large faces polished; the thin faces are sandblasted as described in Ref. [6]. Also shown is a ballistic path of a thermal phonon from the silicon substrate through a thin film as modeled in the MC simulations.

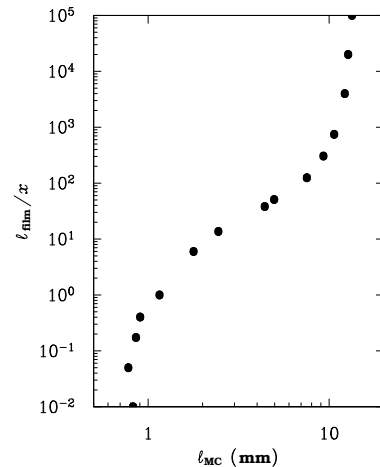


FIG. 12. Typical plot of ℓ_{film}/x versus ℓ_{MC} where x is the film thickness. Normalizing ℓ_{film} with respect to x allows the same plot to be used for different film thicknesses as long as the sample and clamp geometry has not changed (see text for details). The actual code of the Monte Carlo programs may be found in Ref. [39].

corresponding ℓ_{film}/x ; multiplying by x then yields the desired value, ℓ_{film} , that directly corresponds to the measured ℓ_{exp} .

In order to use Fig. 12 as above, the film-substrate sample must be mounted as shown in Fig. 11. Furthermore, the four thin sides of the high purity silicon substrate must be completely roughened (by sandblasting, for example) while the two wide faces must be smooth from Syton polishing, for example), as explained in Ref. [6]. Any film of thickness x must cover both wide faces entirely and uniformly. The height of the sample above the top of the base clamp should be 44.5 mm, the width of the sample 7 mm, and the thickness of the substrate 0.279 mm. The height of the heater, cold thermometer, and hot thermometer clamp above the top of the base clamp should be 41 mm, 4 mm, and 25 mm, respectively. The two interfaces between the heater clamp and the sample (areas of contact) should each be of dimensions $0.279 \times 2 \text{ mm}^2$ while the four interfaces between the thermometer clamps and the sample should each be $0.279 \times 1.5 \text{ mm}^2$. The effect of varying these details are discussed in Ref. [6].

-
- [1] X. Liu, E. J. Thompson, B. E. White, Jr., and R. O. Pohl, Phys. Rev. B **59**, 11767 (1999).
 - [2] A. K. Raychaudhuri and R. O. Pohl, Phys. Rev. B **46**, 10657 (1992).
 - [3] W. A. Phillips, Rep. Prog. Phys. **50**, 1657 (1987).
 - [4] P. A. Medwick, B. E. White, Jr., and R. O. Pohl, J. Alloys and Compounds **270**, 1 (1998).
 - [5] K. A. Topp and D. G. Cahill, Z. Phys. B **101**, 235 (1996).
 - [6] P. D. Vu, J. R. Olson, and R. O. Pohl, J. Low Temp. Phys. **113**, 123 (1998).
 - [7] X. Liu, P. D. Vu, R. O. Pohl, F. Schiettekatte, and S. Roorda, Phys. Rev. Lett. **81**, 3171 (1998).
 - [8] W. Kern, RCA Eng. **28**, 99 (1983).
 - [9] Recipe given by staff at the Cornell Nanofabrication Facility, Ithaca, New York, and dubbed “Piranha-etch”.
 - [10] X. Liu, R. O. Pohl, S. Asher, and R. S. Crandall, J. Non-cryst. Solids **227-230**, 407 (1998).
 - [11] T. Klitsner and R. O. Pohl, Phys. Rev. B **36**, 6551 (1987).
 - [12] G. S. Kumar, G. Prasad, and R. O. Pohl, J. Mat. Sci. **28**, 4261 (1993).
 - [13] D. G. Cahill, Rev. Sci. Instrum. **61**, 802 (1990).
 - [14] X. Liu and R. O. Pohl, Phys. Rev. B **58**, 9067 (1998).
 - [15] C. L. Spiel and R. O. Pohl, Rev. Sci. Instr. (to be submitted).
 - [16] P. W. Anderson, B. I. Halperin, and C. M. Varma, Philos. Mag. **25**, 1 (1972).
 - [17] W. A. Phillips, J. Low Temp. Phys. **7**, 351 (1972).
 - [18] J. Jäckle, Z. Phys. B **257**, 212 (1972).
 - [19] N. W. Ashcroft and N. D. Mermin, *Solid State Physics* (Saunders College, Philadelphia, 1976), p.458.
 - [20] E. T. Swartz and R. O. Pohl, Rev. Mod. Phys. **61**, 605 (1989).
 - [21] G. L. Olson and J. A. Roth, Mat. Sci. Rep. **3**, 1 (1988).
 - [22] R. C. Weast, ed., *CRC Handbook of Chemistry and Physics 67* (CRC Press, Inc., Boca Raton, Florida, 1986), p.E-43.
 - [23] D. Williamson, S. Roorda, M. Chicoine, R. Tabti, P. A. Stolk, S. Acco, and F. W. Saris, Appl. Phys. Lett. **67**, 226 (1995).
 - [24] J. S. Custer, M. O. Thompson, D. C. Jacobson, J. M. Poate, S. Roorda, W. C. Sinke, and F. Spaepen, Appl. Phys. Lett. **64**, 437 (1994).
 - [25] S. Roorda, W. C. Sinke, J. M. Poate, D. C. Jacobson, S. Dierker, B. S. Dennis, D. J. Eaglesham, F. Spaepen, and P. Fuoss, Phys. Rev. B **44**, 3702 (1991).
 - [26] G. Schrag, M. Rebmann, C. Wurster, F. Zeller, K. Lassmann, and W. Eisenmenger, Phys. Stat. Sol. (a) **168**, 37 (1998).
 - [27] F. Zeller, K. Lassman, and W. Eisenmenger, Physica B **263-264**, 108 (1999).
 - [28] W. Wasserbäch, Phys. Stat. Sol. **128**, 55 (1991).
 - [29] N. S. Sokolov, N. L. Yakovlev, and J. Almeida, Solid State Commun. **76**, 883 (1990).
 - [30] K. Krebs, private communication.
 - [31] E. Thompson, P. D. Vu, and R. O. Pohl, Phys. Rev. B (in press).
 - [32] R. C. Zeller and R. O. Pohl, Phys. Rev. B **4**, 2029 (1971).
 - [33] W. Duffy, Jr., J. Appl. Phys. **68**, 5601 (1990).
 - [34] P. G. Klemens, *Encyclopedia of Physics*, vol. 14, S. Flügge, ed., (Springer Verlag, Berlin, 1956) p. 198.
 - [35] R. Berman and D. K. C. MacDonald, Proc. Roy. Soc. **A211**, 122 (1952).
 - [36] P. Lindenfeld and W. B. Pennebaker, Phys. Rev. **127**, 1881 (1962).
 - [37] H. von Löhneysen and F. Steglich, Z. Phys. B **29**, 89 (1978).
 - [38] E. Thompson and R. O. Pohl, Mat. Res. Soc. Symp. Proc. **562** (1999), in press.
 - [39] P. D. Vu, *Phonon Scattering in Thin Films Below 1 K*, Ph.D. thesis, Cornell University (1999).